JOURNAL OF MAGNETIC RESONANCE **128,** 1–11 (1997)
ARTICLE NO. MN971214

The Continuous Wavelet Transform, an Analysis Tool for NMR Spectroscopy

D. Barache,*,†,[1] J-P. Antoine,*,[1] and J-M. Dereppe†,[2]

*Institut de Physique Théorique and †Laboratoire de Chimie Physique et Cristallographie, Université Catholique de Louvain, B-1348 Louvain-la-Neuve, Belgium

Received January 7, 1997; revised June 12, 1997

The discrete wavelet transform has been used in NMR spectroscopy by several authors. We show here that the continuous wavelet transform (CWT) is also an efficient tool in that context. After reviewing briefly the analysis of spectral lines with the CWT, we discuss two applications specific to NMR, namely the removal of a large unwanted line and the rephasing of a signal perturbed by eddy currents. More details on the CWT are given in two appendixes. © 1997 Academic Press

1. INTRODUCTION

A NMR signal or a FID s may be modeled by a linear superposition of spectral lines

$$s(t) = \sum_l s_l(t), \qquad [1.1]$$

where each spectral line s_l has the form

$$s_l(t) = A_l(t)e^{i(\omega_l t+\phi(t))}. \qquad [1.2]$$

The amplitude a_l is directly proportional to the density of nuclei l which have a resonance pulsation ω_l. Ideally the phase ϕ should be constant, but some dynamical effects can influence the signal and make the phase vary in time.

Classically, a NMR signal is visualized by its Fourier spectrum; nevertheless it has been shown that in some cases it is preferable to work in the time domain (*1, 2*). The time analysis is based on a model function for the amplitudes a_l and it assumes that the phase ϕ is constant in time. But in dynamic NMR spectroscopy or in the presence of eddy currents, the phase may suffer some time perturbation. In such a case, the use of a time-frequency analysis seems natural. The method presented here is based on the continuous wavelet transform (CWT). This technique was originally introduced in geophysics (analysis of microseisms used in oil prospection), but by now it has pervaded many sectors of physics, mathematics, and engineering. It has been applied in particular to the analysis of spectral lines in general (*3*) and its application to NMR spectroscopy was also suggested and tested in (*3, 4*). For a general survey of the wavelet method, we refer to (*5, 6*) or the elementary review (*7*).

In a recent paper, Neue (*8*) has emphasized the interest of the wavelet transform in dynamic NMR spectroscopy. More precisely, he proposes to use the discrete wavelet transform (DWT) to extract the dynamical behavior of a NMR signal. However, it seems to us that the CWT is more efficient for this kind of problem for two reasons. First, the CWT, because of its redundancy, is a good tool for analysis and feature determination while the DWT is well adapted for data compression and signal synthesis (see Appendix A). Second, the method used in this paper is supported by some rigorous results (see Appendix B and Note added in proof).

The paper is organized as follows. In Sections 2 to 4, we introduce the CWT and we present briefly the method described in (*3, 6*) for the analysis of spectral lines and asymptotic signals. In Sections 5 and 6, we present two applications of the CWT: the removal of a large spectral line and the rephasing of a NMR signal influenced by eddy currents. Further mathematical information is given in the appendixes.

2. THE CONTINUOUS WAVELET TRANSFORM

The continuous wavelet transform (see Appendix A for the mathematical background) is a mathematical tool which permits one to decompose a signal in terms of elementary contributions called wavelets. These wavelets are obtained from a single function ψ by translations and dilations,

$$\psi_{(b,a)}(t) = \frac{1}{a}\,\psi\left(\frac{t-b}{a}\right), \qquad [2.1]$$

where the parameters of translation, $b \in \mathbb{R}$, and dilation, a

[1] E-mail: [antoine, barache]@fyma.ucl.ac.be.
[2] To whom correspondence should be addressed. E-mail: dereppe@cpmc.ucl.ac.be.

1090-7807/97 $25.00

> 0, may be continuous or discrete. The CWT of a signal s with the analyzing wavelet ψ is the convolution of s with a scaled and conjugated wavelet $\psi_a(t) = \overline{\psi(-t/a)}/a$:

$$S(b, a) = \psi_a * s(b) = \frac{1}{a} \int \overline{\psi\left(\frac{t-b}{a}\right)} s(t) dt. \quad [2.2]$$

It should be remarked that we use here the so-called L^1-normalization, with a factor $1/a$ in [2.1] and [2.2]. Group-theoretical considerations (see Appendix A) lead to the L^2-normalization, with a factor $1/\sqrt{a}$, which guarantees the unitarity of the CWT, but in fact the normalization is arbitrary. The one chosen here enhances small scales, where the information lies, and is indeed used in most practical applications.

In the Fourier domain, expression [2.2] takes the form

$$S(b, a) = \frac{1}{2\pi} \int \overline{\hat{\psi}(a\omega)} \hat{s}(\omega) e^{i\omega b} d\omega, \quad [2.3]$$

where $\hat{s}$ and $\hat{\psi}$ are the Fourier transforms of the signal s and of the wavelet ψ, respectively. Equations [2.2] and [2.3] show clearly that the wavelet analysis is a time-frequency analysis, or, more properly, a time-scale analysis (the scale parameter a behaves as the inverse of a frequency). In particular, relation [2.3] shows that the CWT of a signal s is a filter with a constant relative bandwidth $\Delta\omega/\omega = \text{const}$. If we require the wavelet ψ to satisfy the so-called admissibility condition, namely

$$c_\psi \equiv 2\pi \int |\hat{\psi}(\omega)|^2 \frac{d\omega}{|\omega|} < \infty, \quad [2.4]$$

then the CWT may be inverted exactly and we obtain a reconstruction formula:

$$s(t) = c_\psi^{-1} \iint \psi_{(b,a)}(t) S(b, a) \frac{dadb}{a}. \quad [2.5]$$

A necessary (and almost sufficient) condition for admissibility is that the wavelet have no DC component:

$$\hat{\psi}(0) = 0 \Leftrightarrow \int \psi(t) dt = 0. \quad [2.6]$$

This transform is very general in the sense that there is one CWT for each choice of the analyzing wavelet ψ. For each application, one should select an analyzing wavelet adapted to the type of signal at hand. For instance, in order to detect and to characterize the singularities of a signal (*9*) or a curve (*10*), it is advantageous to use as analyzing wavelet a derivative of the Gaussian. In our case, NMR signals are relatively well defined in frequency, so it is more interesting to use analyzing wavelets which are well localized in frequency space.

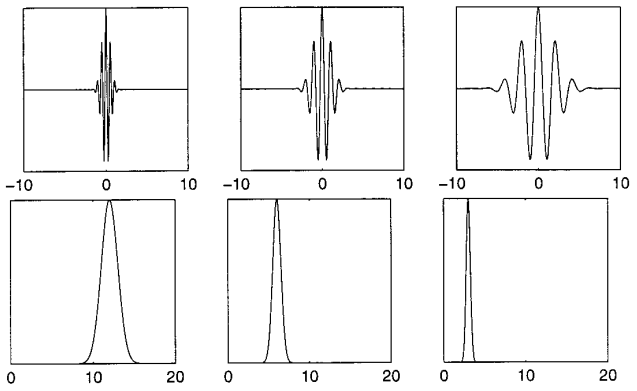

FIG. 1. Support properties of the Morlet wavelet ψ_M: For $a = 0.5$, 1, 2 (left to right), ψ_{ab} has width 3, 6, 12, respectively (top), while $\hat{\psi}_{ab}$ has width 3, 1.5, 0.75, and peaks at 12, 6, 3 (bottom).

This is the case of the Morlet wavelet, defined by

$$\psi(t) = e^{i\omega_0 t} e^{-t^2/(2\sigma_0^2)} + \eta(t),$$
$$\hat{\psi}(\omega) = \sqrt{2\pi}\sigma_0 e^{-(\omega-\omega_0)^2\sigma_0^2/2} + \hat{\eta}(\omega), \quad [2.7]$$

where the correction term η is necessary to enforce the admissibility condition (in the following we shall use the value $\sigma_0 = 1$). If $\omega_0\sigma_0$ is sufficiently large (typically $\omega_0\sigma_0 > 5.5$), then η is numerically negligible. The Morlet wavelet can be interpreted as a bandpass linear filter centered around $\omega = \omega_0/a$ of weight $1/(\sigma_0 a)$ (Fig. 1). All the results presented here have been obtained with the Morlet wavelet, but they can easily be generalized to any analyzing wavelet whose Fourier transform has a single maximum at $\omega = \omega_0$, or to the Gabor transform (STFT) (*3*).

3. SPECTRAL LINES

Let s be a signal of the form

$$s(t) = \sum_{l=1}^{N} s_l(t), \quad [3.1]$$

where $s_l(t) = A_l(t)\exp i\omega_l t$ is the lth spectral line, which has a constant frequency $f_l = \omega_l/2\pi$. Its CWT is given by

$$S(b, a) = \sum_{l=1}^{N} S_l(b, a), \quad [3.2]$$

where S_l, the CWT of s_l, is

$$S_l(b, a) = \frac{1}{2\pi} \int \hat{\psi}(a\omega) \hat{A}_l(\omega - \omega_l) e^{i\omega b} d\omega \quad [3.3]$$

$$= \frac{1}{2\pi} e^{i\omega_l b} \int \hat{\psi}(a(\omega + \omega_l)) \hat{A}_l(\omega) e^{i\omega b} d\omega. \quad [3.4]$$

Using the Taylor expansion of the Fourier transform of the analyzing wavelet, $\hat{\psi}$, around the pulsation ω_l,

$$\hat{\psi}(a(\omega + \omega_l)) = \hat{\psi}(a\omega_l) + \sum_k \frac{(a\omega)^k}{k!} \frac{d^k\hat{\psi}}{d\omega^k}(a\omega_l), \quad [3.5]$$

we obtain the following expansion for S_l:

$$S_l(b, a) = \hat{\psi}(a\omega_l)s_l(b) + e^{i\omega_l b} \sum_{k\geqslant 1} \frac{(-ia)^k}{k!} \frac{d^k\hat{\psi}}{d\omega^k}(a\omega_l) \frac{d^k A_l}{db^k}(b). \quad [3.6]$$

So one has

$$S_l(b, a) \simeq \hat{\psi}(a\omega_l)s_l(b), \quad [3.7]$$

up to first order, and

$$S(b, a) \simeq \sum_{l=1}^{N} \hat{\psi}(a\omega_l)s_l(b). \quad [3.8]$$

If the values of the frequencies ω_l are sufficiently far away from each other, the factor $\hat{\psi}(a\omega_l)$ will allow one to treat each spectral line independently. In this case, the contribution of the lth spectral line to $S(b, a)$ is localized on the scale $a_l = \omega_0/\omega_l$ and, along the line of maxima $a = a_l$, called the lth *ridge* (R_l), the CWT is approximately proportional to the lth spectral line:

$$\frac{S(b, \omega_0/\omega_l)}{\hat{\psi}(\omega_0)} \simeq s_l(b). \quad [3.9]$$

If some frequencies are too close to each other, one can choose ω_0 sufficiently large so as to enforce the resolution of the wavelet in the Fourier space. But, increasing the central frequency of the analyzing wavelet increases the values of the derivatives appearing in [3.6] so that the approximation [3.9] is no longer valid. In this case, the method consists in detecting the resonance pulsation ω_l (by using the Fourier spectrum or the algorithm described in (*3*)) and solving the following system of equations:

$$S(b, \omega_0/\omega_l) = \sum_{m=1}^{N} \hat{\psi}\left(\frac{\omega_0\omega_m}{\omega_l}\right) s_m(b), \quad l = 1, \ldots, N. \quad [3.10]$$

According to Eq. [3.9], the CWT gives a decomposition of the signal s into its components. In a first approximation, each component s_l is detected by the corresponding line of local maxima or *ridge* in the wavelet transform, and along the lth maxima line the CWT is approximately proportional to s_l. The set of all the ridges is called the *skeleton* of the CWT. This time-frequency decomposition can be used to estimate the characteristic parameters of a FID. In the ideal case, each component of the FID can be modeled by

$$s_l(t) = A_l e^{-d_l t} e^{i\omega_l t}, \quad [3.11]$$

where A_l is the real-valued amplitude, d_l the damping factor, and ω_l the resonance pulsation. From Eq. [3.9], the lth spectral line is proportional to the CWT at the scale a_l, so the amplitude along the ridge must verify

$$\ln|s_l(t)| = \ln\left|\frac{S(t, a_l)}{\hat{\psi}(\omega_0)}\right| = -d_l t + \ln A_l. \quad [3.12]$$

As an example, we show in Fig. 2 a synthetic FID with two components, its Fourier transform, its CWT (modulus and phase), and its decomposition into individual components. From this decomposition, we extract A_1, d_1 and A_2, d_2 (Fig. 2c).

The wavelet transform gives a time-frequency decomposition of the signal. So, in the case of noisy data, the effect of the noise is also spread in the time-frequency plane. Accordingly, Donoho uses the DWT to denoise data (*11*). The idea is to threshold the wavelet coefficients before reconstructing the data set. In our case, the noise, even if it is spread, makes difficult the extraction of the ridges. So, it may be interesting to use a model function like [3.11] and to consider as a priori knowledge the fact that the amplitude of the CWT along a ridge behaves according to Eq. [3.12]. Work in that direction is in progress.

4. ASYMPTOTIC SIGNALS

The result given by Eq. [3.9] can be generalized (*3, 6*) to a signal [3.1], where each component has the form

$$s_l(t) = A_l(t)e^{i\phi_l(t)}, \quad [4.1]$$

provided the components s_l are asymptotic, i.e.,

$$\left|\frac{1}{A_l(t)}\frac{dA_l(t)}{dt}\right| \ll \left|\frac{d\phi_l(t)}{dt}\right|. \quad [4.2]$$

Let us define the instantaneous frequency of the lth component (this makes sense if s_l is asymptotic) as

$$f_l(t) = \frac{1}{2\pi}\frac{d\phi_l(t)}{dt}. \quad [4.3]$$

Then, as before, we define a *ridge* R_l, which is approximately a line of local maxima (for a more precise definition, see Appendix B), such that:

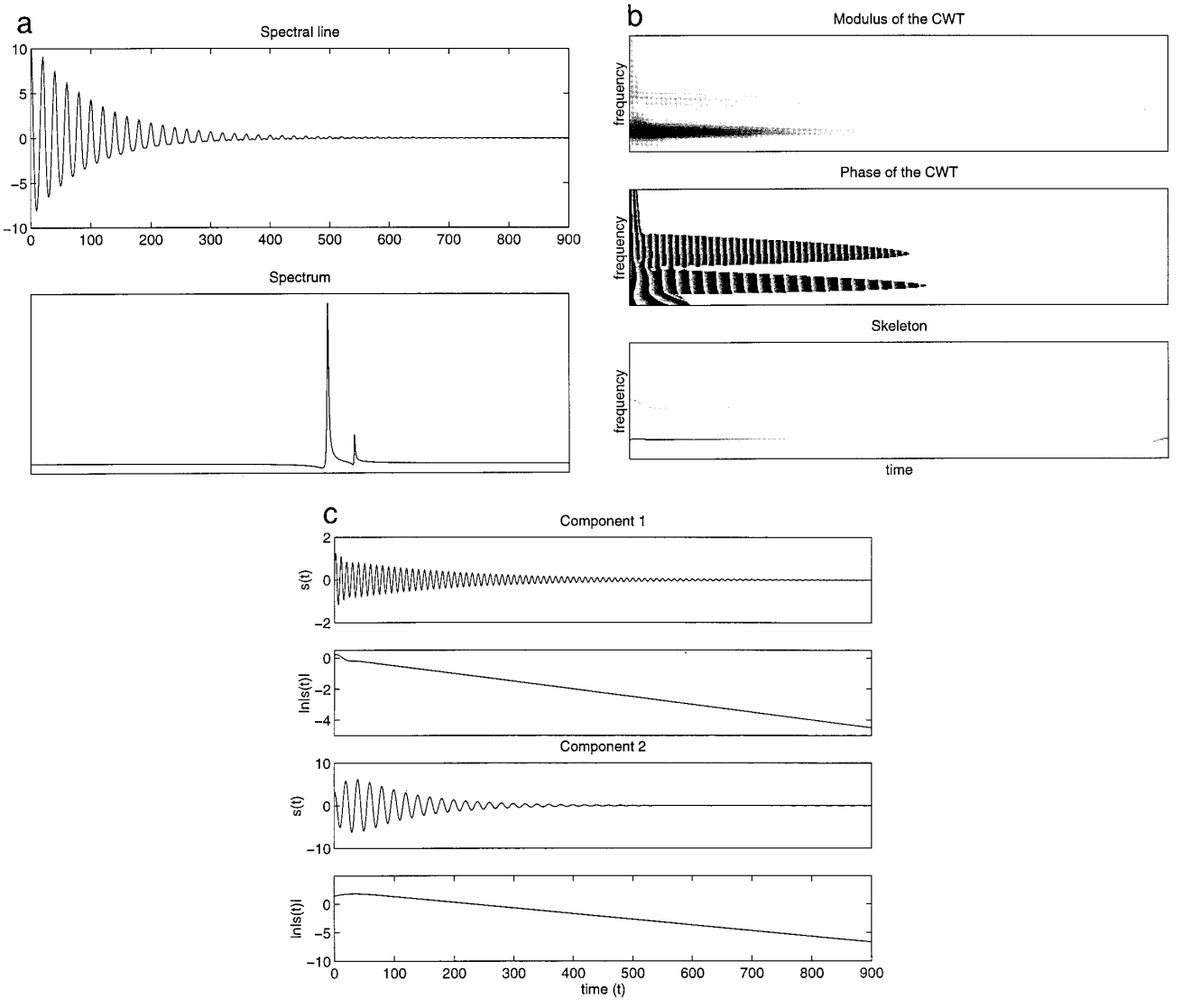

FIG. 2. CWT decomposition of a FID with two components: (a) the FID and its spectrum; (b) modulus, phase, and skeleton of the CWT of the FID; (c) the CWT along the two previous ridges gives the components of the FID. For each component, the logarithm of the amplitude is plotted. The line slopes give the damping factors, $d_1 = 1/200$ (top) and $d_2 = 1/100$ (bottom), and the values at the origin the logarithm of the real-valued amplitudes, $A_1 = 1$ (top) and $A_2 = 10$ (bottom).

1. (*detection*) if the scale $a_l \in R_l$, then the instantaneous frequency is

$$f_l(b) = \frac{1}{2\pi} \frac{\omega_0}{a_l(b)}; \qquad [4.4]$$

2. (*characterization*) along the ridge R_l, the CWT is approximately proportional to the component s_l (if $\hat{\psi}$ is sufficiently localized),

$$S(b, a_l(b)) \simeq d_\psi(b) s_l(b), \quad a_l(b) \in R_l, \qquad [4.5]$$

where the correction term d_ψ depends only on the analyzing wavelet ψ.

The aim of this method is to separate the different spectral lines of a signal s and to extract their time behavior. However, a good localization in frequency is necessary in order to separate the lines, whereas a good localization in time is required for extracting the time behavior of each line. The balance between these two conflicting requirements gives the limits of the method. Note, however, that more adaptive algorithms have been proposed recently for obtaining a better approximation (*12*).

As an example, let us take a signal with an oscillating frequency:

$$s(t) = \exp(i(\omega_c t + \beta \cos(\omega_1 t))) = A(t) e^{i\phi(t)}. \qquad [4.6]$$

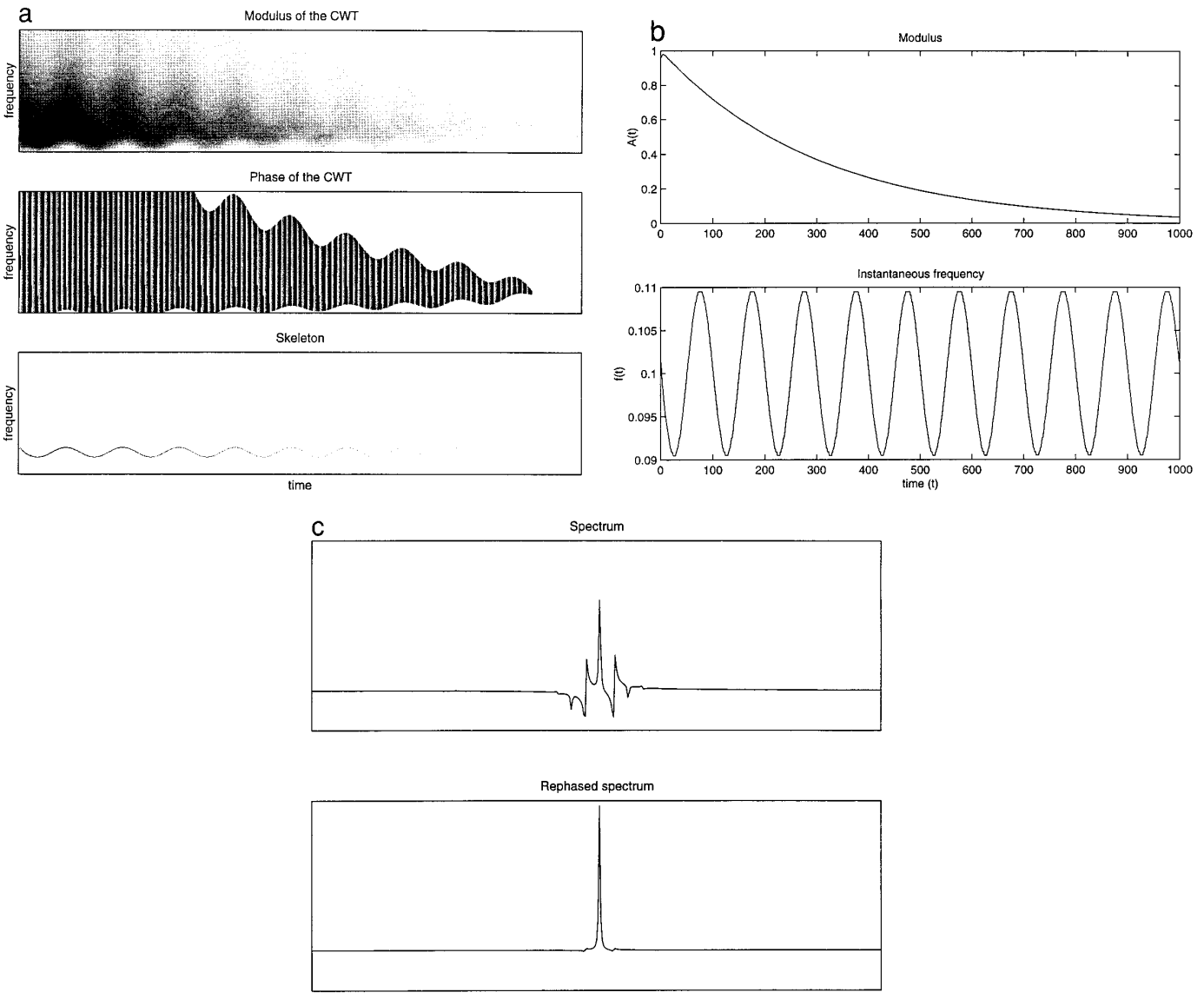

FIG. 3. Extraction of the instantaneous frequency and correction of the spectrum of the signal [4.6] with $\omega_c = 2\pi * 0.1$, $\beta = 1$, $\omega_1 = 2\pi * 0.01$: (a) modulus, phase, and skeleton of the CWT; (b) modulus and instantaneous frequency of the signal extracted from the ridge. c) Spectrum of the signal before and after the phase correction extracted from the phase of the CWT along the ridge.

This kind of signal, which modelizes the FID of a rotating crystal, has been treated also by Neue (*8*) with the help of the DWT. Figure 3 represents its CWT (modulus and phase) and the maxima of the modulus (Fig. 3a), the modulus $A(t)$ and the instantaneous frequency $f(t)$ of the signal extracted from the maxima (Fig. 3b), and the spectrum of the signal before and after the correction explained in the next section (Fig. 3c).

5. REMOVAL OF A LARGE SPECTRAL LINE

In some spectra, such as spectra of polymers or proteins, a large spectral line precludes an easy and quantitative observation of important small lines. An interesting application of the CWT is to subtract this large component from the other ones. Let ω_1 be the resonance frequency of this line (it can be evaluated from the Fourier spectrum directly or from the CWT by an algorithm described in (*4*)). The CWT at the scale $a_1 = \omega_0/\omega_1$ is given by

$$s_1^{(1)}(t) = \frac{S(t, a_1)}{\bar{\psi}(\omega_0)} \simeq A_1(t)e^{i\omega_1 t} + \Delta S(t, a_1). \quad [5.1]$$

The second term in [5.1] is a sum over the other spectral lines, with the amplitudes attenuated by the exponential factor.

In order to extract only the desired spectral line, one can iterate the procedure with $s_1^{(1)}$ as the new input signal. Then the error term becomes negligible after a certain number of iterations. Thus the first component is completely characterized and can be removed from the initial signal. An example of the remarkable efficiency of this procedure is given in Fig. 4 (see also (*3, 4*)). The material is polyethylene and the huge line is the CH_2 peak, which completely obliterates the fine details (top). After subtraction of the large peak (bottom), the smaller lines become clearly identifiable. The remarkable fact is that these small lines have not been perturbed nor displaced by the subtraction procedure, only slightly attenuated. The reason, of course, is that they live at a scale completely different from that of the CH_2 peak, and the two are therefore completely decoupled by the CWT.

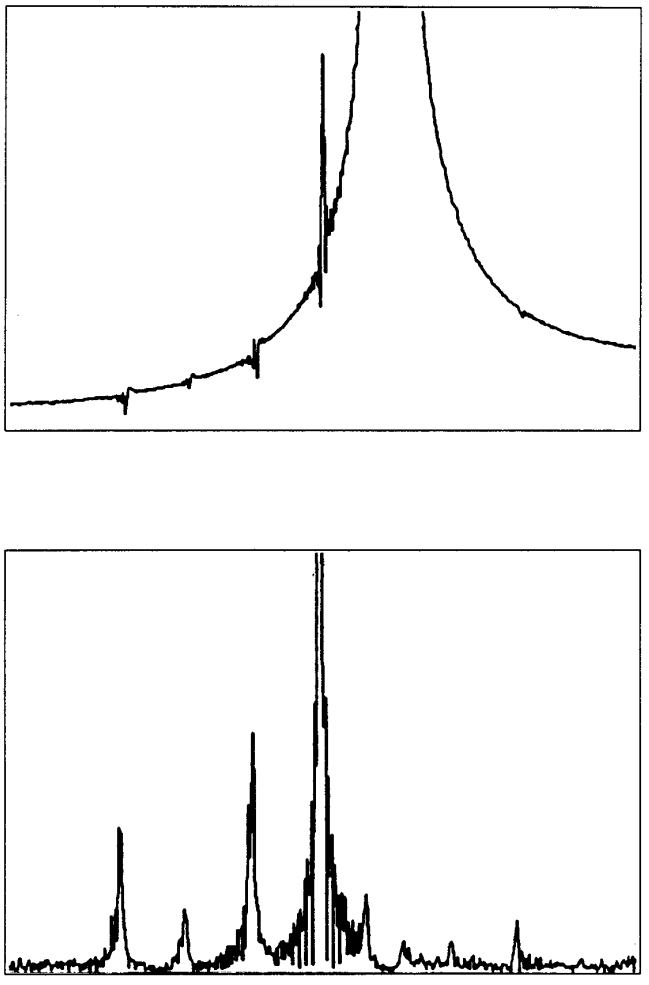

FIG. 4. Subtraction of a large spectral line: (a) the original spectrum, from polyethylene, in the vicinity of the large CH_2 peak; (b) the reconstructed spectrum after subtraction of the CH_2 peak.

6. DYNAMICAL PHASE CORRECTION

Pulsed magnetic field gradient NMR is now a standard technique for studying both diffusive and coherent molecular motions.

Unfortunately, the switching of large amplitude gradients used in this method gives rise to a number of problems. Gradient switching can induce mechanical vibration and/or eddy currents both in the probe and in the magnet. These effects depend on the timing and amplitude of the gradients and therefore introduce large errors in the measurement of diffusion coefficients. Several techniques, such as delaying the acquisition or using shielded gradients, have been proposed in order to alleviate the problem.

However, the use of a magnetic field gradient pulse normally generates a time-dependent B_0 field caused by the eddy current in the bore tube and the uncorrected FID or echo produces spectra with major distortions. An experimental method (*1, 13*) has been proposed for eliminating the problem; it consists in extracting the time behavior of the phase from a test signal in order to correct the other signals. However, both the production of an appropriate test signal and the extraction of the time dependence of its phase are difficult and expensive operations. We show here that the CWT can be used for removing the distortions introduced by gradient switching *without* using a test signal, thus simplifying the procedure considerably.

As shown in Section 4, the CWT may be used for extracting the time behavior of the phase from the signal itself. The proof of this result consists in rephasing the spectra of the acquired signals.

A NMR signal detected from the nth nuclear spin can be modeled by

$$s_n(t) = A_n(t)e^{i(\omega_n t+\phi(t))}, \qquad [6.1]$$

where the effect of the eddy currents lies in the time dependence of the phase ϕ. As we have seen in Section 4, the CWT is given along the nth ridge by [4.5]. Thus the phase of the CWT along this ridge is expressed by

$$\Phi(b, a_n(b)) \equiv \arg[S(b, a_n(b))] \qquad [6.2]$$

$$= \omega_n b + \phi(b) + \arg[d_\Psi(b)], \qquad [6.3]$$

where $d_\Psi(b)$ is given in Appendix B. Then the rephased signal is simply

$$s^{(r)}(t) = s(t)e^{-i(\Phi(t,a_n(t))-\arg[d_\Psi(t)])} \qquad [6.4]$$

$$= \sum_l A_l(t)e^{i(\omega_l-\omega_n)t}, \qquad [6.5]$$

where the nth component is chosen as a reference spectral line.

First, we treat a spectacular example where the time dependence of the B_0 field is known. The entire spectrum of

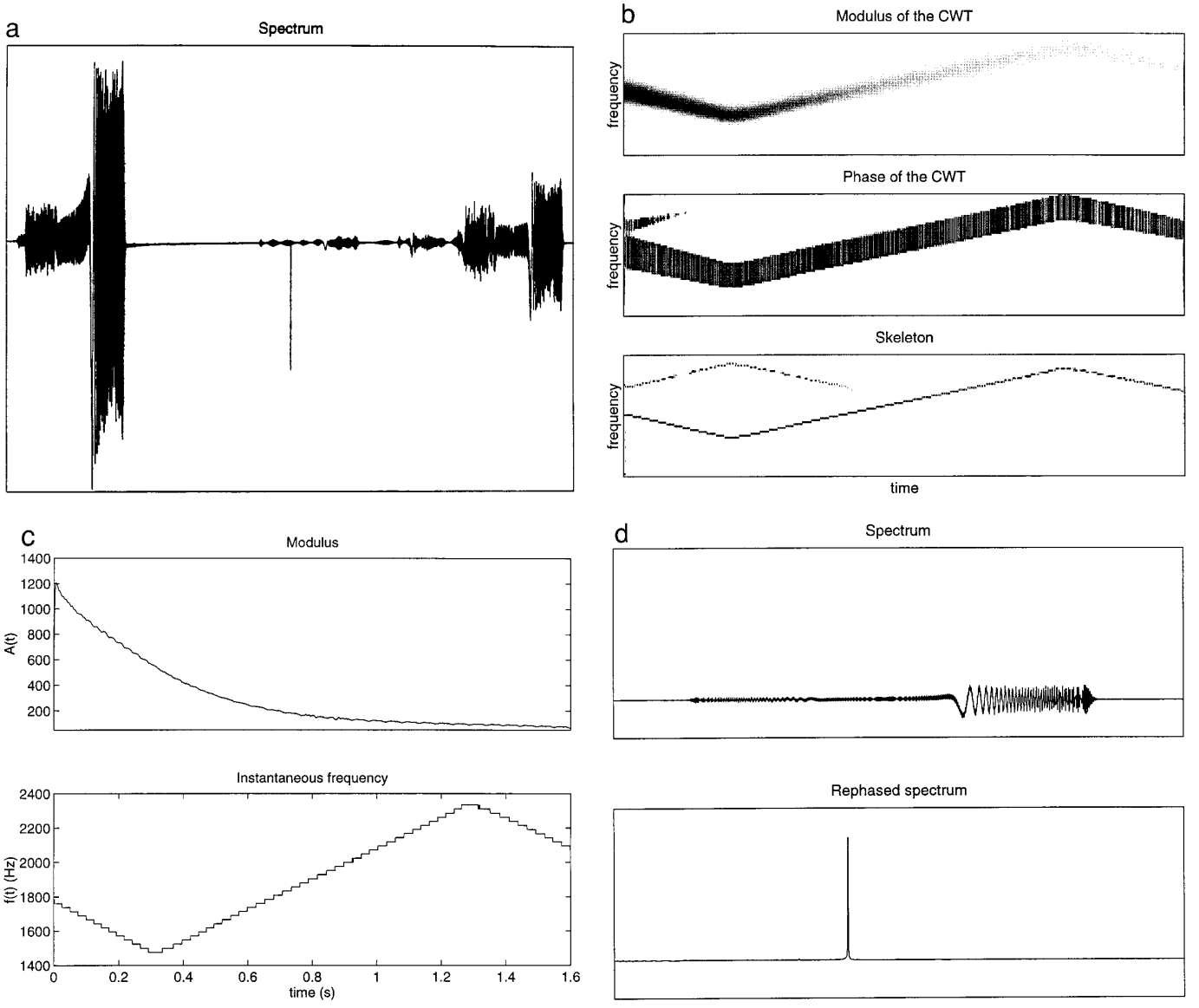

FIG. 5. FID perturbed by a linear time-dependent field superimposed on the static field: (a) spectrum; (b) modulus, phase, and skeleton of the CWT around the chloroform line (left line in (a)); (c) modulus and instantaneous frequency of the chloroform line extracted from the ridge; (d) spectrum around the chloroform line before (top) and after rephasing (bottom).

the distorted FID is presented in Fig. 5a. The CWT around the chloroform line (left line in Fig. 5a) is used to extract the time-dependent variation of the frequency (Figs. 5b and 5c) and so the time dependence of the B_0 field. The other line seen in the modulus of the CWT (Fig. 5b (top)) corresponds to the mirror images of the TMS line (right line in Fig. 5a) resulting from a misadjustment of the quadrature detection. As a proof, the rephased spectrum around the chloroform line is shown in Fig. 5d.

Figure 6 presents four spectra of NMR signals acquired on a Bruker MSL 300 equipped with a microimaging unit system, at a constant time of 2 ms after the switching off of a 4-ms gradient pulse of various decreasing amplitudes (successively 530, 330, 100, and 33 mT/m). For each signal, the CWT allows the extraction of the time behavior of the phase and the rephasing of the spectrum.

The last example is a FID with two spectral lines perturbed by the switching of a magnetic field gradient (Fig. 7 (top)). The FID is rephased with the phase of first line (left) extracted by using the CWT. The non-Lorentzian shape of the rephased spectrum (Fig. 7 (middle)) is explained by the fact that the switching affects not only the phase but also the modulus of each component. As a proof, the FID is reconstructed by fitting the modulus of each component with a damping exponential (Fig. 7 (bottom)).

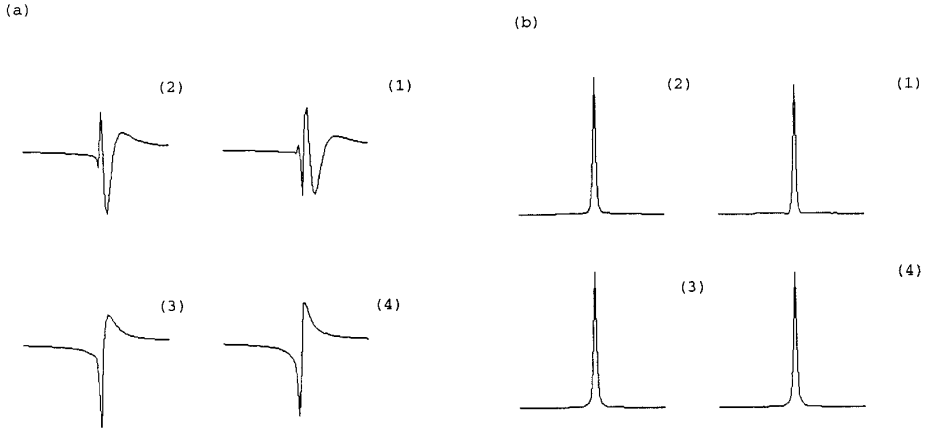

FIG. 6. Correction of four FIDs perturbed by the switching of magnetic field gradients of decreasing amplitudes (successively 530 (1), 330 (2), 100 (3), and 33 (4) mT/m): (a) spectra of the FID before correction; (b) spectra after a phase correction deduced from the phase of the CWT along the ridge.

7. CONCLUDING REMARKS

The wavelet transform (CWT or DWT) gives a time-frequency representation of a signal. This representation has proved to be particularly useful in dynamic NMR spectroscopy (*8*).

The discrete character of the DWT explains its popularity in the signal processing community (ease of implementation). But the analysis is constrained to a fixed set of discrete scales (or frequencies). Numerically, the CWT can be obtained in a straightforward way from the discrete Fourier transform by applying a discretized version of Eq. [2.3]. Namely, it suffices to estimate the discretized Fourier transform version of the analyzing wavelet at each scale, multiply the two spectra, and take an inverse (fast) Fourier transform. So the choice of the discrete scales is free and can be adapted to the problem. The method presented here uses explicitly the redundancy of the CWT to analyze the signals. Then the useful information is extracted from the entire time-frequency plane by using the concept of ridges introduced in (*3*). This method, which is approximative, has the advantage of being supported by some rigorous results (see Appendix B).

Finally, we have discussed two applications: suppression of a large unwanted spectral line and rephasing a spectrum perturbed by a time-dependent magnetic field. As far as we know, the latter is the first real application of the wavelet transform in dynamic NMR spectroscopy. Another potential application, already suggested by Neue (*8*), would be the study of very fast chemical reactions where the composition of the reactant evolves within the acquisition time of the FID. Work on this subject is in progress.

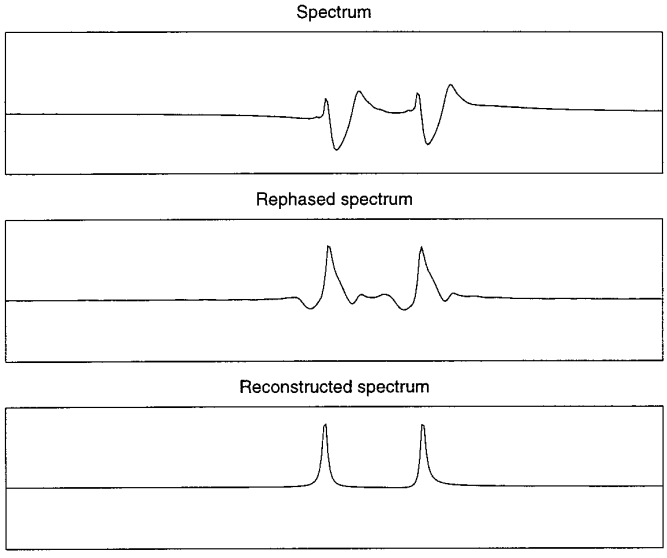

FIG. 7. Correction of a FID with two components perturbed by the switching of a magnetic field gradient: spectrum (top), rephased spectrum (middle), and the reconstructed spectrum (bottom).

APPENDIX A

The Mathematics of the CWT

Let ψ be an analyzing wavelet, i.e., a function $\psi \in L^2(\mathbb{R})$ satisfying the admissibility condition [2.4]. Given a signal $s \in L^2(\mathbb{R})$, its CWT with respect to ψ is given by Eqs. [2.2] and [2.3].

Then a straightforward calculation shows that this transform conserves energy (in the sense of signal processing), that is,

$$\iint |S(b, a)|^2 \frac{dadb}{a^2} = c_\psi \int_{-\infty}^{\infty} |s(t)|^2 dt. \quad [A.1]$$

In other words, the CWT is an isometry from the space of signals onto a closed subspace H_ψ of $L^2(\mathbb{R}^2_+, dadb/a^2)$, where $\mathbb{R}^2_+$ denotes the scale-position half-plane $\mathbb{R}^2_+ = \{(b, a), b \in \mathbb{R}, a > 0\}$. Therefore, the CWT may be inverted on its range H_ψ by the adjoint map—and this gives precisely the reconstruction formula [2.5]. The latter may also be interpreted as an expansion of the signal into the wavelets $\psi_{(b,a)}$, with (wavelet) coefficients $S(b, a)$.

A second important fact is the so-called reproduction property. Indeed it may be shown that the orthogonal projection P_ψ from $L^2(\mathbb{R}^2_+, dadb/a^2)$ onto the closed subspace H_ψ (the space of wavelet transforms) is an integral operator, with kernel

$$K(b', a'; b, a) = c_\psi^{-1}\langle \psi_{(b',a')} | \psi_{(b,a)} \rangle. \qquad [A.2]$$

In other words, a function $f \in L^2(\mathbb{R}^2_+, dadb/a^2)$ is the WT of some signal iff it satisfies the reproduction identity

$$f(b', a') = \iint K(b', a'; b, a) f(b, a) \frac{dadb}{a^2}. \qquad [A.3]$$

For this reason, K is called the *reproducing kernel* of ψ. It is also the autocorrelation function ψ and as such it plays an essential role in calibrating the CWT (*7*).

Remark. Notice that the measure $dadb/a^2$ on $\mathbb{R}^2_+$ is invariant under dilations and translations. This is no accident. Indeed the CWT may be derived by considering the group "$ax + b$" of dilations and translations of the real line. The relation $[U(b, a)\psi](t) = a^{1/2}\psi_{(b,a)}(t)$ defines a unitary representation of this group in the space $L^2(\mathbb{R})$ of signals, and this representation is *square integrable*, which means that there exists nonzero functions $\psi \in L^2(\mathbb{R})$ such that the matrix element $\langle U(b, a)\psi | \psi \rangle$ is square integrable with respect to the invariant measure $dadb/a^2$. These are precisely the admissible wavelets, since a direct calculation shows that

$$\iint |\langle U(b, a)\psi | \psi \rangle|^2 \frac{dadb}{a^2} = c_\psi \|\psi\|^2; \qquad [A.4]$$

i.e., ψ is admissible iff $c_\psi < \infty$. All the properties of the CWT described above follow from these facts (*5*, *7*).

Now relation [A.3] shows that the CWT is enormously redundant (the signal has been unfolded from one variable t to two variables (b, a)). Thus it is not surprising that all the information is already contained in a small subset of the values of $S(b, a)$. The skeleton is an example of such a subset. Another example is obtained by taking an appropriate discrete subset $\Gamma = \{a_j, b_k\}$ of the half-plane $\mathbb{R}^2_+$, as it is necessary in any case for numerical evaluation of the integrals. However, for most wavelets ψ, the resulting family $\{\psi_{(a_j,b_k)}\}$ is *never* an orthogonal basis (for the Morlet wavelet, for instance, the kernel K is a Gaussian; thus it never vanishes). At best, it is an overcomplete set of vectors, technically called a *frame*, provided that Γ contains sufficiently many points (*5*).

Notice that the discretized CWT which is used in practice, including in the present paper, is totally different from the so-called *discrete WT* (DWT) that we now describe. Indeed, orthogonal bases of wavelets may be constructed, but from a completely different approach. One starts with a *multiresolution analysis*, that is, an increasing sequence $\{V_j, j \in \mathbb{Z}\}$ of closed subspaces of $L^2(\mathbb{R})$ such that:

(1) $\cap_{j\in\mathbb{Z}} V_j = \{0\}$ and $\cup_{j\in\mathbb{Z}} V_j$ dense in $L^2(\mathbb{R})$;
(2) $f(t) \in V_j \Leftrightarrow f(2t) \in V_{j+1}$;
(3) there exists a function $\phi \in V_0$, called a *scaling function*, such that the family $\{\phi(t - k), k \in \mathbb{Z}\}$ of its integer translates is an o.n. basis of V_0.

Condition (2) means that no scale is privileged. Combining (2) and (3), one gets an orthonormal basis of V_j, namely $\{\phi_{j,k}(t) \equiv 2^{j/2}\phi(2^j t - k), k \in \mathbb{Z}\}$.

Each V_j can be interpreted as an approximation space. The approximation of $f \in L^2(\mathbb{R})$ at the resolution 2^j is defined by its projection onto V_j. The additional details needed for increasing the resolution from 2^j to 2^{j+1} are given by the projection of f onto the orthogonal complement W_j of V_j in V_{j+1},

$$V_j \oplus W_j = V_{j+1}, \qquad [A.5]$$

and we have, for any $j_0 \in \mathbb{Z}$,

$$V_{j_0} \oplus \left(\bigoplus_{j \geqslant j_0} W_j \right) = \bigoplus_{j\in\mathbb{Z}} W_j = L^2(\mathbb{R}). \qquad [A.6]$$

Then the theory asserts the existence of a function ψ, called the *mother* of the wavelets, explicitly computable from ϕ, such that $\{\psi_{j,k}(t) \equiv 2^{j/2}\psi(2^j t - k), k \in \mathbb{Z}\}$ is an orthonormal basis of V_j, and thus $\{\psi_{j,k}(t), j, k \in \mathbb{Z}\}$ is an orthonormal basis of $L^2(\mathbb{R})$. These are the *orthonormal wavelets*. However, the elements of that basis can seldom be obtained analytically; they tend to be highly irregular functions (sometimes nowhere differentiable or fractal). They are in fact obtained in an indirect fashion, through the theory of filters familiar in signal processing (see (*5*) for further details).

One may notice that this version of the WT, called the *discrete* or *dyadic* WT (DWT), is very rigid, and this explains why several generalizations have been proposed (biorthogonal wavelets, wavelet packets, $\cdots$), which are more flexible and hence more suitable for applications.

We emphasize that the DWT is totally different in spirit from the CWT, either truly continuous or discretized, and they have complementary ranges of applications:

• in the CWT, there is a lot of freedom in choosing the wavelet ψ, but one does not get an orthonormal basis, at best a frame. This is a tool for analysis and feature determination—as in NMR spectroscopy, or other problems where the scaling properties of the signal are unknown a priori, for instance, in fractal analysis (*14*).

• in the DWT, one insists on having an orthonormal basis, but the wavelet is *derived* from the postulated scaling function ϕ that generates the multiresolution analysis. Together with the generalizations mentioned above, this is the preferred tool for data compression and signal synthesis, and the most popular in the signal processing community.

More radically, one may even say that the kind of problems treated here can be solved only with the CWT, that the DWT is simply not adapted to the underlying physics. For instance, the algorithm for detecting spectral lines, as well as the ridge concept, rests upon a stationary phase argument. Similarly, the determination of fractal exponents exploits the scaling behavior of homogeneous functions or distributions and the covariance properties of the CWT. All these notions are foreign to the DWT, which is more a signal processing tool, as used in electrical engineering, and a very powerful one.

APPENDIX B

The Case of General Asymptotic Signals

Let us consider a signal of the form

$$s(t) = \sum_l s_l(t), \qquad [B.1]$$

where each component $s_l(t) = A_l(t)\exp(i\phi_l(t))$ is asymptotic.

In the text, we have discussed in detail the case of the sum of spectral lines ($\phi_l'(t) = \omega_l$). The result can be adapted directly to the case where the instantaneous frequencies are approximatively constant ($\phi_l''(t) \simeq 0$). The wavelet transform of s is approximately given by Eqs. [3.2] and [3.6], where the constant frequency ω_l is replaced by the instantaneous frequency $\phi_l'(b)$. In this approximation, each component of s is given by a maxima line of its CWT and the term d_ψ in Eq. [4.5] is constant, $d_\psi(b) = \hat{\psi}(a_l(b)\phi_l'(b)) = \sqrt{2\pi}$. The approximation used for the spectral lines is based on the asymptotic expansion of the amplitude of the signal and it is justified when the instantaneous frequencies are constant or quasi-constant.

At the other extreme, if the amplitudes are constant and the instantaneous frequencies vary in time, it is more convenient to use the stationary phase approximation (*3, 6*). The wavelet transform of s_l, with the Morlet wavelet, is expressed by

$$S_l(b, a) = \frac{1}{a}\int A_l(t) e^{-(1/2)(t-b)/a)^2} e^{i(\phi_l(t) - \omega_0((t-b)/a))}\, dt. \qquad [B.2]$$

In this approximation, the modulus $M_l(b, a)$ and the phase $\Psi_l(b, a)$ of S_l are given, respectively (*3, 12*), by

$$M_l(b, a) = |S_l(b, a)| = A_l(t_s(a)) \frac{\sqrt{2\pi}}{(1 + a^4\phi_l''^2(t_s))^{1/4}} \times \exp\left(-\frac{1}{2}\frac{(b - t_s(a))^2 a^2 \phi_l''^2(t_s)}{1 + a^4\phi_l''^2(t_s)}\right) \qquad [B.3]$$

and

$$\Psi_l(b, a) = \arg(S_l(b, a)) = \phi_l(t_s(a)) - \omega_0\left(\frac{t_s(a) - b}{a}\right) + \frac{1}{2}\arctan(a^2\phi_l''(t_s)) + \frac{1}{2}(b - t_s(a))^2 \cdot \frac{\phi_l''(t_s)}{1 + a^4\phi_l''^2(t_s)}, \qquad [B.4]$$

where the stationary points $t_s(a)$ are such that

$$\frac{d\phi_l}{dt}(t_s) = \frac{\omega_0}{a}. \qquad [B.5]$$

On the set of points where $t_s(a) = b$, Eqs. [B.3] and [B.4] simplify considerably. This set of points is defined as a *ridge*, R_l, of the CWT. On a ridge, the wavelet transform is directly related to the component s_l of s,

$$S_l(b, a_l(b)) = \frac{\sqrt{2\pi}\, e^{i/2 \arctan(-a_l'(b)\omega_0)}}{(1 + a_l(b)'^2\omega_0^2)^{1/4}} s_l(b) = d_\Psi(b) s_l(b), \qquad [B.6]$$

where $a_l(b)$ is the scale on the ridge R_l at the time b and $a_l'(b) = da_l(b)/db$. The ridge of the CWT is not exactly a maxima line, because of the term $(1 + a^4\phi_l''^2(t_s))^{1/4}$ in Eq. [B.3], which depends on the scale a. Thus another method is necessary for extracting the ridge. It is easy to show that the points such that $t_s(a) = b$ verify the relations

$$\frac{d\Psi_l(b, a)}{db} = \frac{\omega_0}{a}. \qquad [B.7]$$

This equation gives a necessary condition for a point (a, b) to be on the ridge R_l, and it can be used for extracting it.

The estimation of the different asymptotic components s_l can be improved by combining the two methods. In this case, the equation which permits extracting the ridge is more complicated (*12*).

Note added in proof. After this paper was submitted for publication, another article appeared (*15*), in which the authors discuss in detail the

application of the CWT to NMR quantification problems, by the method developed in (*3, 4*) and used here. That paper is complementary to the present one.

ACKNOWLEDGMENTS

D. Barache is supported by EC Human Capital and Mobility Contract ERBCHRXCT 940432. He acknowledges the hospitality of the Institut de Physique Théorique and the Laboratoire de Chimie Physique et de Cristallographie of the Université Catholique de Louvain, and he is grateful to A. Jacques, A. van den Boogaart, and P. Vandergheynst for fruitful discussions.

REFERENCES

1. A. van den Boogaart, The use of signal processing algorithms to obtain biochemically relevant parameters from magnetic resonance data set, Ph.D. thesis, University of London at St. George's Hospital Medical School (1995).

2. R. de Beer and D. van Ormondt, Analysis of NMR data using time domain fitting procedures, *in* ''In-vivo Magnetic Resonance Spectroscopy. I. Probeheads, Radiofrequency Pulsed, Spectrum Analysis'' (M. Rudin, Guest Ed.), NMR Basic Principle and Progress Series, Vol. 26, pp. 201–248, Springer-Verlag, Berlin/Heidelberg (1992).

3. N. Delprat, B. Escudié, Ph. Guillemain, R. Kronland-Martinet, Ph. Tchamitchian, and B. Torrésani, Asymptotic wavelet and Gabor analysis: Extraction of instantaneous frequencies, *IEEE Trans. Inform. Theory* **38,** 644–664 (1992).

4. Ph. Guillemain, R. Kronland-Martinet, and B. Martens, Estimation of spectral lines with the help of the wavelet transform: Application in NMR spectroscopy linear time-frequency representation, *in* ''Wavelets and Applications'' (Y. Meyer, Ed.), pp. 38–60, Masson, Paris, and Springer-Verlag, Berlin (1991).

5. I. Daubechies, ''Ten Lectures on Wavelets,'' SIAM, Philadelphia (1992).

6. B. Torrésani, ''Analyse continue par ondelettes,'' Savoirs Actuels, InterEditions, CNRS Editions, Paris (1995).

7. J-P. Antoine, Wavelet analysis: A new tool in signal processing, *Phys. Mag.* **16,** 17–42 (1994).

8. G. Neue, Simplification of dynamical NMR spectroscopy by wavelet transform, *Solid State Nucl. Magn. Reson.* **5,** 305–314 (1996).

9. J-F. Muzy, E. Bacry, and A. Arnéodo, Multifractal formalism for fractal signals: The structure function approach versus the wavelet-transform modulus-maxima method, *Phys. Rev. E* **47,** 875–884 (1993).

10. J-P. Antoine, D. Barache, R. M. Cesar Jr., and F. L. da Costa, Multiscale shape analysis using the continuous wavelet transform, *in* ''Proceedings IEEE International Conference on Image Processing (ICIP-96), Lausanne, Switzerland, Sept. 1996'' (P. Delogne, Ed.), Vol. I, pp. 291–294, IEEE, Piscataway, NJ (1996); Shape characterization with the wavelet transform, *Signal Proc.* **62** (1997) to appear.

11. D. Donoho, Nonlinear wavelet methods for recovery of signals, densities, and spectra from indirect and noisy data, *in* ''Different Perspectives on Wavelets, Proceedings of Symposia in Applied Mathematics'' (I. Daubechies, Ed.), Vol. 47, pp. 173–205, Amer. Math. Soc., Providence, RI (1993).

12. Ph. Guillemain and R. Kronland-Martinet, Characterization of acoustics through continuous linear time-frequency representation, *Proc. IEEE* **84,** 617–643 (1996).

13. R. J. Ordidge and I. D. Cresshull, The correction of transient b_0 field shifts following the application of pulsed gradient by phase correction in the time domain, *J. Magn. Reson.* **69,** 151–155 (1986).

14. A. Arnéodo, F. Argoul, E. Bacry, J. Elezgaray, E. Freysz, G. Grasseau, J. F. Muzy, and B. Pouligny, Wavelet transform of fractals, *in* ''Wavelets and Applications'' (Y. Meyer, Ed.), pp. 286–352, Masson, Paris, and Springer-Verlag, Berlin (1991).

15. H. Serrai, L. Senhadji, J. D. de Certaines, and J-L. Coatrieux, Time-domain quantification of amplitude, chemical shift, apparent relaxation time T_2^*, and phase by wavelet-transform analysis. Application to biomedical magnetic resonance spectroscopy, *J. Magn. Reson.* **124,** 20–34 (1997).